Title

The bHLH transcription factor MpHYPNOS is a critical regulator of gemma dormancy in the liverwort *Marchantia polymorpha*.

Authors

Hirotaka Kato[1,5,*], Nami Yoshimura[1,*], Mikako Yoshikawa[1], Arisa Yasuda[1], Hideyuki Matsuura[2], Kosaku Takahashi[3], Daisuke Takezawa[4], Tomoyuki Furuya[1], Yuki Kondo[1], Hidehiro Fukaki[1], Tetsuro Mimura[1,3], Kimitsune Ishizaki[1]

Addresses

[1]Graduate School of Science, Kobe University, Kobe, Hyogo 657-8501, Japan

[2]Research Faculty of Agriculture, Hokkaido University, Sapporo, Hokkaido, 060-8589, Japan

[3]Faculty of Applied Bioscience, Tokyo University of Agriculture, Tokyo, 156-8502, Japan

[4]Graduate School of Science and Engineering, Saitama University, Saitama 338-8570, Japan

[5]Present address: Graduate School of Science and Engineering, Ehime University, Matsuyama, Ehime 790-8577, Japan

[*]These authors equally contributed.

Author for correspondence

Kimitsune Ishizaki

Telephone: +81 78-803-5727

Email: kimi@emerald.kobe-u.ac.jp

Total word count: 4,519

Word count for each section

Introduction: 732

Materials and Methods: 1,281

Results: 1,542

Discussion: 964

Number of figures: 5 (all should be published in colour)

Number of tables: 0

Number of supporting information: 9

Summary

- Dormancy is a key process for land plants to adapt drastically changing terrestrial environment. The liverwort *Marchantia polymorpha* produce dormant propagules called gemmae for asexual reproduction. The plant hormone abscisic acid (ABA) plays significant roles in the regulation of dormancy in both seed of flowering plants and gemma of *M. polymorpha*.
- Based on the previous transcriptome analysis, here we identified the basic helix-loop-helix transcription factor MpHYPNOS (MpHYP), as a key regulator of gemma dormancy.
- The knock-out mutants showed much higher germination rate of gemmae in gemma cup than ABA-related mutants did, while the growth and development were the same as wild type. Transient induction of MpHYP caused irreversible growth arrest in gemma and thallus. Transcriptome and qRT-PCR analyses revealed that MpHYP repressed cell-cycle related genes and induced the ABA biosynthesis and responsive genes. Indeed, ABA amounts were increased or decreased by overexpression or knock-out of Mp*HYP*, respectively. However, the growth arrest caused by MpHYP overexpression was not suppressed by the mutation in the ABA receptor gene.
- These data suggest that MpHYP regulates gemma dormancy and thallus growth partially through the ABA pathway. Our findings would provide the clues to understand ABA-dependent and independent regulation of dormancy in land plants.

Key words

ABA, bHLH, Cell cycle, Dormancy, Gemma, *Marchantia polymorpha*

Introduction

Dormancy is a key process for land plants to adapt drastically changing terrestrial environment. Land plants produce stress-tolerant and dormant reproductive units such as seeds and spores. Their growth is arrested until specific physiological and environmental signals are perceived, and such delay of germination allow them to withstand unfavorable conditions such as drought or low temperature, and to disperse themselves to distant location via winds, water flows, or animals. In addition to sexual reproduction through spores, the liverwort *Marchantia polymorpha* propagate asexually by producing gemmae inside gemma cups which is formed on dorsal side of vegetative body, thallus. Gemmae are dormant when they are in gemma cup (Shimamura, 2016). Once gemmae fall out by physical reason such as rain drops, they start germination in the presence of light and water (Bowman, 2016). Previous studies presented that gemma dormancy is regulated by several plant hormones; abscisic acid (ABA), auxin, and ethylene (Eklund *et al.*, 2015; Kato *et al.*, 2015; Eklund *et al.*, 2018; Li *et al.*, 2020). ABA plays major roles in initiation and maintenance of seed dormancy in flowering plants (Sano & Marion-Poll, 2021), and thus it was proposed that land plants share common mechanisms to regulate dormancy of progeny (Eklund *et al.*, 2018). Auxin also plays a positive role in dormancy of seed and gemmae (Liu *et al.*, 2013; Eklund *et al.*, 2015). The mutants of auxin biosynthesis and signaling produced germinated gemmae inside gemma cups (Eklund *et al.*, 2015; Kato *et al.*, 2017). On the other hand, ethylene plays opposite roles in dormancy regulation of seed and gemmae. While ethylene and its signaling factors promote release of seed dormancy in dicot species [reviewed in (Longo *et al.*, 2020)], ethylene application enhances gemma dormancy in gemma cup (Li *et al.*, 2020).

Studies in flowering plants have revealed basis of biosynthesis pathway and signaling mechanism of ABA [reviewed in (Sano & Marion-Poll, 2021)]. Conversion from zeaxanthin to all-*trans*-violaxanthin by zeaxanthin epoxidase [ZEP; (Marin *et al.*, 1996)] encoded by Arabidopsis *ABA1* gene is widely recognized as the first step of ABA biosynthesis. ABA4 is important for conversion from all-trans-violaxanthin into 9'-*cis*-violazanthin or 9'-*cis*-neoxanthin, although enzymatic activity of ABA4 has not been shown (Perreau *et al.*, 2020). The first dedicated step in ABA biosynthesis is production of xanthoxin by a 9-cis-epoxycarotenoid dioxygenase [NCED; (Schwartz *et al.*, 1997)].

Xanthoxin is then converted by a xanthoxin dehydrogenase (XD) into abscisic aldehyde (Gonzalez-Guzman *et al.*, 2002), which is oxidized into ABA by an abscisic aldehyde oxidase [ABAO; (Seo *et al.*, 2000)]. ABA signal is perceived by soluble receptors, PYRABACTIN RESISTANCE 1 (PYR1)/PYR1-LIKE (PYL)/REGULATORY COMPONENTS OF ABA RECEPTORS (RCAR), and inhibits the phosphatase activity of group A protein phosphatase 2C (PP2C-A) (Ma *et al.*, 2009; Park *et al.*, 2009). In the absence of ABA, PP2C-A directly inactivates subclass III SNF1-related protein kinase 2 (SnRK2) through dephosphorylation (Umezawa *et al.*, 2009; Vlad *et al.*, 2009). SnRK2s activate ABA response by phosphorylation of target proteins including bZIP transcription factor ABA INSENSITIVE 5 [ABI5; (Nakashima *et al.*, 2009)].

Phylogenomic studies revealed that the components of ABA biosynthesis and signaling are basically conserved across the land plants (Komatsu *et al.*, 2020). *M. polymorpha* produces endogenous ABA (Li *et al.*, 1994; Tougane *et al.*, 2010), and has single orthologs of biosynthetic genes except for XD (Bowman *et al.*, 2017). Exogenously supplied ABA cause growth inhibition, accumulation of soluble sugar represented by sucrose, enhancement of desiccation tolerance, and activate stress-related genes including *Late Embryogenesis Abundant-Like* (*LEAL*) genes (Tougane *et al.*, 2010; Akter *et al.*, 2014; Jahan *et al.*, 2019). Such responses are not occurred in the loss-of-function mutants of Mp*PYL1* which encodes the major ABA receptor expressed in vegetative tissues (Jahan *et al.*, 2019). Constitutive expression of PP2C-A (MpABI1) and knock-out of downstream transcription factor (MpABI3A) also cause ABA insensitivity and defect in gemma dormancy (Eklund *et al.*, 2018).

Here, we identified the basic helix-loop-helix (bHLH) transcription factor MpHYPNOS (MpHYP) playing a critical role in gemma dormancy. MpHYP belongs to class VIIIb bHLH family which includes *A. thaliana* INDEHICHENT (IND) and HECATEs (HECs). IND and HEC play diverse roles including gynoecium development, but little is known about their function in dormancy regulation. Transcriptome analyses and hormone quantification revealed that MpHYP promotes gemma dormancy partially through the regulation of ABA biosynthesis and responses. Our study provides evolutionary insights of class VIIIb bHLH function and cooperation of ABA-dependent and -independent dormancy regulation in land plants.

Materials and Methods

Plant materials, growth conditions, and transformations

Male and female accessions of wild type *M. polymorpha*, Takaragaike-1 (Tak-1) and Tak-2 (Ishizaki *et al.*, 2008), were maintained asexually. *M. polymorpha* plants were cultured as previously described (Yasui *et al.*, 2019) unless otherwise defined. Dexamethasone (DEX), cycloheximide (CHX) and ABA were solved in ethanol to make stock solutions, and added into the agar medium after autoclaving. Agrobacterium-mediated transformations into sporelings or thalli were performed as previously described (Ishizaki *et al.*, 2008; Kubota *et al.*, 2013).

Generation of knock-out mutants of Mp*HYP*

4.5 kb or 4.8 kb of genomic region surrounding the region encoding bHLH domain were amplified using the promoter sets MpHEC1_5IF_F and MpHEC1_5IF_R, or MpHEC1_3IF_F and MpHEC1_3IF_R, and cloned into *Pac*I or *Asc*I site of pJHY-TMp1 vector, respectively (Ishizaki *et al.*, 2013). The resultant plasmid was used for transformation of F1 sporelings generated by crossing Tak-2 and Tak-1. To confirm recombination, genomic PCR was performed using the primer sets A (MpHEC1_GT_check_5_F and MpEF_GT_R1), B (H1F and MpHEC1_GT_check_3_R), and C (MpHEC1_5IF_check_F and MpHEC1_3IF_check_R). Sex determination was performed by genomic PCR with the mixture of four primers, rbm27_F, rbm27_R, rhf73_F, and rhf73_R.

Complementation of Mp*hyp*^{ko}

The genomic fragment from 4.3 kb upstream of transcriptional start site to the last codon of Mp*HYP* was amplified using the primer set of MpHEC1_pro_F and MpHEC1_CDS_nsR, and cloned in to the pENTR/D-TOPO vector (Thermo Fisher), followed by LR reaction with pMpGWB301 (Ishizaki *et al.*, 2015) using LR Clonase II Enzyme Mix (Thermo Fisher). This plasmid was then transformed into Mp*hyp*^{ko} thalli, but phenotypic complementation was not observed (data not shown). Then the downstream genomic fragment was amplified using the primer set of MpHEC1_CDS_IF_F and MpHEC1_3UTR_IF_R2, and integrated with In-Fusion HD

Cloning Kit (Clontech) using *BamH*I and *Asc*I sites, followed by transformation into Mp*hyp*^{ko} thalli.

Overexpression of Mp*HYP*

Coding sequence without stop codon was amplified from Tak-1 cDNA using the primer set of MpHEC1_CDS_F and MpHEC1_CDS_nsR, and cloned into pENTR/D-TOPO (Thermo Fisher), followed by the LR reaction with pMpGWB313 (Ishizaki *et al.*, 2015) to fuse with Mp*EF1α* promoter and glucocorticoid receptor domain (GR). The resultant plasmid was used for transformation of Tak-1 thalli.

Mutagenesis of Mp*NCED*

Two oligo DNAs (NY009 and NY010) were annealed and cloned in pMpGE_En03 (Sugano *et al.*, 2018). The resultant cassettes expressing sgRNA and Cas9 were transferred into pMpGE010 using LR Clonase II Enzyme Mix (Thermo Fisher), and then transformed into Tak-1 thalli. To check the sequence of Mp*NCED* locus, genomic region around sgRNA target site was amplified using the primer set NY019 and NY020, and sequenced.

Mutagenesis of Mp*PYL1* locus in Mp*HYP-GR* plants

The plasmids expressing sgRNA targeting Mp*PYL1* and Cas9 (Jahan *et al.*, 2019) were transformed into Mp*HYP-GR* thalli. To check the sequence of Mp*PYL1* locus, genomic region around sgRNA target site was amplified using the primer set MpPYL1_qPCR_L1 and MpPYL1_qPCR_R1, and sequenced.

Measuring germination rate of gemmae in gemma cups

Gemmae isolated from gemma cups located at the most basal position in thalli were stained by 15 μM propidium iodide solution supplemented with 0.01% Triton X-100 for 15 min and observed under the binocular fluorescent microscope M205 FA (Leica) using the filter set for DsRED. The number of gemmae with elongated rhizoids were counted. 79 – 114 gemmae were used for each data point of three biological replicates.

Scanning electron microscopy

For scanning electron microscopy (SEM), thalli were frozen in liquid nitrogen and observed with a scanning electron microscope VHX-D500 (KEYENCE).

Promoter activity assay

6.3 kb genomic fragment including 4.3 kb upstream of translational start site was amplified from Tak-1 genomic DNA using the primer set of MpHEC1_pro_F and MpHEC1_pro_R, and cloned into pENTR/D-TOPO vector. Promoter fragment was then transferred into pMpGWB304 (Ishizaki *et al.*, 2015) to fuse with GUS. Resultant plasmid was introduced into Tak-1 thalli using Agrobacterium-mediated method (Kubota *et al.*, 2013). Histochemical assays for GUS activity were performed as described previously with slight modifications (Ishizaki *et al.*, 2012). Plant tissues were vacuum-infiltrated followed by incubation in the GUS assay solution for 4 h. To obtain section images, samples were embedded in Technovit 7100 plastic resin as previously described (Yasui *et al.*, 2019). Semi-thin sections (8-mm thickness) were obtained with a microtome (HM 335E, Leica Microsystems, Germany) for light microscopy and stained with 0.01 % (w/v) Safranin O (Waldeck GmbH & Co. KG). Sections were observed with an upright microscope BX51 (OLYMPUS) equipped with a CMOS camera DP74 (OLYMPUS).

Quantitative RT-PCR

Total RNA was extracted using RNeasy Plant Mini Kit (QIAGEN), and reverse-transcribed using ReverTra Ace qPCR RT Master Mix with gDNA remover (TOYOBO) according to the manufacture's protocol. Quantitative PCR was performed with the Light Cycler 96 (Roche) using KOD SYBR qRT-PCR Mix (TOYOBO). The primers used in this study are listed in Table S1. Transcript levels of each gene was normalized by that of MpEF1α (Saint-Marcoux *et al.*, 2015). Each measurement was performed with three or four biological replicates and three technical replicates.

RNA-seq

Total RNA was isolated using RNeasy Plant Mini Kit (QIAGEN) with manufacture's protocol. The extracted RNA was treated with an RNase-free DNase set (QIAGEN), and purified with RNeasy MinElute Cleanup Kit (QIAGEN). For the RNA samples from gemma cups of WT and Mp*hyp*^{ko}, the sequence libraries were constructed with TruSeq

RNA Sample Preparation Kit (Illumina) and sequenced with Hiseq 4000 (Illumina) to obtain 100 bp paired-end data. For Mp*HYP-GR* with or without 2 h of DEX treatment, the sequence libraries were constructed with TruSeq standard mRNA Library Prep (Illumina) and sequenced with NovaSeq 6000 (Illumina) to obtain 100 bp paired-end data. For Mp*HYP-GR* with or without 24 h of DEX treatment, the sequence libraries were constructed with NEBNext Ultra II RNA Library Prep Kit for Illumina (NEB) and sequenced with Hiseq 4000 (Illumina) to obtain 150 bp paired-end data. All the sequenced raw reads were deposited in DDBJ Sequence Read Archive (DRA) under the project accession number DRA013946.

Quality assessment for raw RNA-seq reads was performed using FastQC (www.bioinformatics.babraham.ac.uk/projects/fastqc). Illumina adapters at the ends of the paired reads were cleaned up using Cutadapt 2.1 (Martin, 2011). The cleaned FASTQ reads were mapped onto the *Marchantia polymorpha* genome (v6.1 accessed through Marpolbase: https://marchantia.info/) using HISAT2 v2.1.0 (Kim *et al.*, 2019) with default parameters. Post-processing of SAM/BAM files was performed using SAMTOOLS v1.9 (Li *et al.*, 2009). GFF file was converted into GTF format using gffread embedded in cufflinks (Trapnell *et al.*, 2010), and then FeatureCounts v1.6.4 (Liao *et al.*, 2014) was used to count the raw reads corresponding to each gene. EdgeR (Robinson *et al.*, 2009) was used to normalize the raw counts and perform the differential expression analysis (Padj < 0.01). Principal component analysis (PCA) was performed using normalized expression data of all genes. GO enrichment analysis was performed using PlantRegMap by converting gene ID from v6.1 to v3.1 (Tian *et al.*, 2019).

EdU incorporation assay

To visualize S-phase cells, the Click-iT EdU Imaging Kit (Life Technologies) was used. EdU staining was performed as described previously (Furuya *et al.*, 2021), with slight modifications. During the sample clearing with ClearSee solution, cell walls were stained with SCRI Renaissance Stain 2200 (1:20,000 dilution). Alexa Fluor555 fluorescence was visualized using the confocal laser scanning microscope FLUOVIEW FV1000 (Olympus) at excitation and detection wavelengths of 559 and 570 – 670 nm, respectively. Z-projection images were created using ImageJ software.

ABA measurement

Plant tissue (ca. 1.0 g) was frozen with liquid nitrogen, crushed, and soaked overnight in 20 mL of ethanol. UPLC separation was performed using a Waters ACQUITY ethylene-bridged (BEH) C18 column (2.1 mm i.d. x 100 mm) and the Waters Micromass Quanttro Premier Tandem Quadrupole Mass Spectrometer (Waters, Milford, MA, USA). The endogenous ABA concentration was analyzed according to the method described previously (Kobayashi *et al*., 2010).

Results

Mp*HYP* plays critical role in gemma dormancy

In the previous study, we compared transcriptome data obtained from whole thalli (TH), midrib (MR) and gemma cup (GC), and identified 10 transcription factors which was highly expressed in GC (Yasui *et al.*, 2019). Among them, Mp5g18910 (Mapoly0073s0051 in ver 3.1 genome) showed the next highest expression in GC relative to that in TH after *GEMMA CUP-ASSOCIATED MYB1* (*GCAM1*) which is a critical regulator of gemma cup formation (Yasui *et al.*, 2019). Confirmation by qRT-PCR presented that Mp5g18910 showed 11.5-fold higher expression in GC than TH (Fig. 1a). Mp5g18910 is composed of a single exon (Fig. 1b), and the encoded protein was phylogenetically classified in class VIIIb basic helix-loop-helix (bHLH) subfamily which contains HECATEs (HECs) and INDEHISCENT (IND) of *A. thaliana* (Bowman *et al.*, 2017; Bonnot *et al.*, 2019). To analyze the biological function of Mp5g18910, we generated the knock-out mutants by the homologous recombination method (Fig. 1b and S1; Ishizaki *et al.*, 2013). We obtained two independent lines (#173 and #182) showing the same phenotype with no obvious defects except for germinated gemmae inside gemma cups (Figs. 1c, d, and S1). At the 17-day-old stage, Tak-1 wild type (WT) gemmae were completely dormant and no elongated rhizoids were observed. In contrast, 27.8% gemmae of Mp*hyp*^{ko} mutant already germinated inside gemma cups (Fig. 1d,e). This dormancy defect was completely rescued by introducing the genomic fragment of Mp5g18910 (Fig. 1e), and thus we defined this gene as Mp*HYPNOS* (Mp*HYP*) named after the personification of sleep in Greek mythology.

Mp*HYP* is expressed in apical notch, midrib, and developing gemma

To understand where Mp*HYP* functions more precisely, we introduced fusion construct of Mp*HYP* promoter region and GUS reporter gene into WT (MpHYP_{pro}:*GUS*). Relatively weak GUS activity was observed around meristematic notch of young (5-day-old) gemmalings (Fig. 2a). At 10-day-old or later stages, strong GUS activity was observed around meristematic notches, apical region of midrib, and GCs (Fig. 2b,c). When we looked into GC, relatively high GUS activity was observed in early developing gemmae and ventral side of thallus (Fig. 2d,e). Interestingly, little GUS activity was

observed in mature gemmae (Fig. 2f). These results suggest that Mp*HYP* is expressed in apical notch, midrib, GC and developing gemma, which is consistent with the RNA-seq and qRT-PCR results (Fig. 1).

Overexpression of Mp*HYP* represses gemma germination and thallus growth

To investigate the effect of Mp*HYP* overexpression, we generated the transgenic plants expressing the fusion protein of MpHYP and glucocorticoid receptor domain (GR) under the control of Mp*EF1α* promoter (Mp*HYP-GR*). MpHYP-GR protein should be active only in the presence of dexamethasone (DEX; Schena *et al.*, 1991). Expression of Mp*HYP* in Mp*HYP-GR* plants were more than 100-fold in comparison with WT (Fig. 3a). When Mp*HYP-GR* plants were grown on DEX-containing medium, not only ungerminated gemmae but also 1-week-old thalli showed severe growth arrest (Fig. 3b,c). Interestingly, when the DEX-treated gemma or thalli were transferred on the mock medium, DEX-treated plants still showed severe growth arrest at least for 1 week (Fig. 3b,c). These results suggest that MpHYP can strongly repress thallus growth as well as gemma germination in irreversible manner.

MpHYP represses cell division activity

To understand downstream pathway of Mp*HYP*, we performed RNA-seq experiments using gemma cups of WT and Mp*hyp*^{ko}, and 1-week-old gemmalings of Mp*HYP-GR* with 2 or 24 h of DEX treatment. Principal component (PC) analysis plot showed each biological replicate closely located, and both PC1 and PC2 values correlated with the direction of genetic manipulation of Mp*HYP* (Fig. 4a). When we compared gemma cups of WT and Mp*hyp*^{ko}, we found that 2,750 and 2,222 genes were up- and down-regulated in Mp*hyp*^{ko}, respectively (Fig. 4b). Then we compared 1-week-old gemmalings of Mp*HYP-GR* incubated with or without DEX for 2 or 24 h. 2,700 or 4,250 genes were up-regulated, while 1,854 or 4,244 genes were down-regulated after 2 or 24 h induction, respectively (Fig. 4b). 1,535 (57%) up-regulated genes and 1,316 (71%) down-regulated genes found in 2 h condition were also up- and down-regulated in 24 h, respectively (Fig. 4b). When we checked the overlap of DEG among the three comparisons, 412 genes were down-regulated in Mp*hyp*^{ko} and up-regulated in Mp*HYP-GR* at both timepoints, and 413 genes behaved oppositely (Fig. 4b). Therefore, we defined them as MpHYP-activated and

MpHYP-repressed genes, respectively, and used them for gene ontology (GO) enrichment analysis to investigate which biological pathway is regulated by MpHYP. While no GO terms were significantly enriched (q-value < 0.01) in MpHYP-activated genes, many GO-terms related to DNA replication were enriched in MpHYP-repressed genes (Fig. 4c). Among known cell cycle-related genes (Bowman *et al*., 2017), four genes encoding cyclins or cyclin-dependent kinase, which are important for cell cycle progression (Komaki *et al*., 2012), were found in MpHYP-repressed genes (Talbe S2). Especially the expression of Mp*CYCD;1*, one of two members of D-type cyclin which have been shown to promote transition from G1 to S phase in angiosperm and moss (Masubelele *et al.*, 2005; Ishikawa *et al.*, 2011), was significantly decreased by induction of Mp*HYP-GR* within 2 h (Fig. 4d, Table S2). Repression of Mp*CYCD;1* by Mp*HYP-GR* was not suppressed by the translation inhibitor cycloheximide (CHX), suggesting that Mp*CYCD;1* is a direct target of Mp*HYP* (Fig. 4d). To confirm whether overexpression of Mp*HYP* repress DNA replication, we performed 5-ethynyl-2'-deoxyuridine (EdU) incorporation assay which visualizes the entry into S phase. While mock treated gemmalings showed around 50 EdU-positive cells per apical notch, DEX treated gemmalings showed little or no EdU-positive cells (Fig. 4e,f). These results suggest that MpHYP repressed cell division activity through the repression of cell cycle-related genes.

<u>MpHYP promotes dormancy partially through ABA pathway</u>

It has been reported that the plant hormones ABA, auxin, and ethylene positively regulate gemma dormancy in *M. polymorpha* (Eklund *et al.*, 2015; Kato *et al.*, 2017; Eklund *et al.*, 2018; Li *et al.*, 2020). To investigate whether these hormones are involved in MpHYP-dependent dormancy regulation, we checked the expression of known genes involved in each hormonal pathway in our RNA-seq data. No ethylene-related genes were found in either of the MpHYP-activated or -repressed genes (Table S3). Among auxin-related genes, Mp*GRETCHEN HAGEN 3A* (Mp*GH3A*: Mp6g07600) encoding an auxin inactivating enzyme was found in MpHYP-repressed genes (Table S4). However, known auxin-activated genes were not found in MpHYP-activated genes. These results suggest that MpHYP does not function through the regulation of auxin and ethylene pathway.

When we focused on ABA-related genes, we found that a putative ABA biosynthesis gene, Mp*ABA4* (Mp6g13390), and 18 Mp*LEAL* genes were MpHYP-

activated (Tables S5 and S6). Although the down-regulation in Mp*hyp*^{ko} is not significant, other 12 Mp*LEAL* genes and two other known ABA-responsive/signaling genes, Mp*ABI3A* and Mp*ABI5B* (Eklund *et al.*, 2018), were significantly up-regulated in Mp*HYP-GR* at both time points (Table S5). Notably, an ABA biosynthesis gene, MpNCED (Mp2g07800), was rapidly and strongly up-regulated in Mp*HYP-GR* in the presence of DEX, which was confirmed by time course qRT-PCR experiments (Fig. 5a; Table S5). On the other hand, Mp*ABA4*, Mp*LEAL1* and Mp*LEAL5* genes were up-regulated only 4 h and later after induction (Fig. 5a). Activation of Mp*NCED* by DEX was not inhibited by the translation inhibitor CHX, while that of Mp*LEAL5* was suppressed (Fig. 5b). These results suggest that MpHYP directly activate Mp*NCED* expression, which results in increase of ABA level and transcriptional responses. To confirm this hypothesis, we measured the change of ABA level by genetic modification of Mp*HYP*. Mp*hyp*^{ko} accumulated lower level of ABA in gemma cup than WT, while DEX treatment on Mp*HYP-GR* thallus caused increase of ABA level (Fig. 5c, d).

To investigate whether ABA-dependent pathway plays major role in Mp*HYP*-dependent gemma dormancy, we compared germination rate of gemmae in WT, Mp*hyp*^{ko}, and ABA receptor mutant Mp*pyl1*^{ge2b} (Jahan *et al.*, 2019). In addition, we generated mutants of Mp*NCED* using CRISPR/Cas9 method (Mp*nced-1*^{ge} and Mp*nced-2*^{ge}; Fig. S2a; Sugano *et al.*, 2018). These mutants have frame shift mutations in the beginning of conserved region, and thus should be loss-of-function allele. Around 30% of gemmae of Mp*hyp*^{ko} mutants were already germinated inside gemma cups on 17-day-old thalli, while most of the gemmae of WT, Mp*yl1*^{ge2b} *and* Mp*nced* mutants were still dormant at the same stage (Fig. 5e). In our experimental condition, significant differences between WT and Mp*pyl1*^{ge2b} or Mp*nced*^{ko} were observed in only much later stage (28-day-old; Fig. S2b). Then we generated loss-of-function mutants of Mp*PYL1* in Mp*HYP-GR* background by the CIRSPR/Cas9 method (Mp*pyl*^{ge}/Mp*HYP-GR* #1 and #2 ; Fig. S3a). Mp*pyl*^{ge}/Mp*HYP-GR* plants were insensitive to exogenously supplied ABA as Mp*pyl1*^{ge2b} mutants in WT background (Fig. S3b; Jahan *et al.*, 2019). Growth arrest caused by DEX treatment was not suppressed by the mutation of Mp*PYL1* (Fig. 5f), suggesting that the contribution of MpPYL1-dependent pathway to gemma dormancy or growth arrest caused by MpHYP is limited. Recent studies presented that there are some ABA-independent pathways to regulate ABA responses through the control of SnRK2s

activities (Saruhashi *et al.*, 2015; Née *et al.*, 2017; Nishimura *et al.*, 2018). To investigate whether similar bypasses are present downstream of MpHYP, we measured the expression of ABA-responsive genes in Mp*pyl1*^{ge}/Mp*HYP-GR* plants. While the expression of Mp*NCED* was activated by DEX treatment regardless of the presence of MpPYL1, that of MpLEAL5 was not induced by DEX in Mp*pyl1*^{ge}/Mp*HYP-GR* plants (Fig. 5g). This suggest that activation of ABA-responsive genes by MpHYP is MpPYL1-dependent.

Discussion

MpHYP is a key regulator of gemma dormancy

Dormancy is a key process to survive a harsh environment on land. The liverwort *M. polymorpha* produces gemma for asexual reproduction, which is dormant in the absence of germination signals including light and water. Previous studies presented that dormancy of gemma is regulated by ABA like seed in angiosperms (Eklund *et al.*, 2018). Based on our previous transcriptome analysis (Yasui *et al.*, 2019), we identified the bHLH-type transcription factor, MpHYP as a critical regulator of gemma dormancy in *M. polymorpha*. MpHYP directly promotes the expression of ABA biosynthesis gene, Mp*NCED*, which results in the increase of ABA content and up-regulation of ABA-responsive genes (Fig. 5, Tables S5-6). However, the lower gemma germination rate of Mp*nced*^{ge} and Mp*pyl1*^{ge} than Mp*hyp*^{ko}, and the same growth arrest phenotype caused by Mp*HYP-GR* regardless with the mutation of Mp*PYL1* gene suggest that contribution of ABA biosynthesis and perception is partial to MpHYP-dependent dormancy regulation. The previous study demonstrated that ABA signal in gemma, not in gemma cup, is important to maintain gemma dormancy (Eklund *et al.*, 2018). Histochemical analysis presented that Mp*HYP* promoter is active in gemma cups and developing gemmae, but not in mature gemmae (Fig. 2). These data suggest that MpHYP is important for the establishment rather than maintenance of gemma dormancy during gemma development and might reflect the limited contribution of ABA pathway.

Besides ABA, auxin and ethylene is known to regulate dormancy of both gemma of *M. polymorpha* and seed of angiosperms (Liu *et al.*, 2013; Corbineau *et al.*, 2014; Eklund *et al.*, 2015; Kato *et al.*, 2017; Li *et al.*, 2020). However, our transcriptome analysis suggest that MpHYP is not likely to function through these pathways. One candidate pathway for MpHYP-dependent dormancy regulation is cell cycle. The present study showed that MpHYP inhibit various cell cycle-related genes and entry into S-phase (Fig. 4, Table S2). Especially, our qRT-PCR with CHX treatment suggest that MpHYP directly down-regulates Mp*CYCD;1*, of which expression was not inhibited by ABA in the previous RNA-seq analyses (Jahan *et al*., 2019). Interestingly, growth arrest caused by transient induction of MpHYP-GR continued for at least one week after the induction was stopped, and this growth inhibition was independent of ABA-pathway (Fig. 3). Such

long-term effect might be achieved through epigenetic modifications. In angiosperms, dramatic changes in chromatin state and epigenetic marks are occurred between dormancy establishment and germination (Lujan-Soto & Dinkova, 2021). Genome-wide or target gene-specific epigenetic analysis would be a key to understand the mechanism for MpHYP functions.

Possible interacting partners of MpHYP

Mp*HYP* is the sole gene encoding class VIIIb bHLH in *M. polymorpha* (Bowman *et al.*, 2017). This class contains *A. thaliana* IND and HEC genes which play critical roles in gynoecium and fruit development (Liljegren *et al.*, 2004; Gremski *et al.*, 2007; Girin *et al.*, 2011; Schuster *et al.*, 2015). Previous studies presented that HEC genes also play important roles in maintenance of shoot apical meristem and phytochrome-dependent photomorphogenesis (Schuster *et al.*, 2014; Zhu *et al.*, 2016; Gaillochet *et al.*, 2017; Kathare *et al.*, 2020). In this study, we demonstrated that MpHYP can both promote or repress the expression of the target genes (Fig. 4d and 5b). Such bifunctionality is probably achieved by the dedicated interacting partners. In general, bHLH transcription factors function by forming dimer with itself or other bHLH proteins. It was reported that IND and HEC interact with other bHLHs such as ALCATRAZ, SPATULA (SPT), and PHYTOCHROM INTERACTING FACTORs (PIFs) (Liljegren *et al.*, 2004; Gremski *et al.*, 2007; Girin *et al.*, 2011; Schuster *et al.*, 2014; Zhu *et al.*, 2016). All of them belong to the class VII bHLH subfamily, which contains only a single *M. polymorpha* gene, MpPIF (Inoue *et al.*, 2016). Gemmae of Mp*pif* mutants show reduced dormancy and germinate even in dark condition or inside gemma cups (Inoue *et al.*, 2016; Hernandez-Garcia *et al.*, 2021), suggesting that MpHYP might function with MpPIF and integrate light and other signals to regulate gemma dormancy. It is noteworthy that HEC proteins negatively regulate PIF function by direct interaction and promote light-dependent seed germination in *A. thaliana* (Zhu *et al.*, 2016), which seems to be opposite relationship between MpHYP and MpPIF. Genetic and physical interaction between them should be carefully investigated in the future study. In addition, the recent study presented that the GRAS-type transcription factor MpDELLA which is the sole member of DELLA family in *M. polymorpha,* represses the activity of MpPIF on gemma dormancy (Bowman *et al.*, 2017; Hernandez-Garcia *et al.*, 2021). Repression of PIF activity by DELLA through

protein interaction is also conserved in flowering plants (de Lucas *et al.*, 2008; Feng *et al.*, 2008). Interestingly, it was also reported that DELLA proteins interact with HEC1 in yeast (Feng *et al.*, 2008; Arnaud *et al.*, 2010; Gaillochet *et al.*, 2018). Identifying the interacting partners of MpHYP would be a key to understand the function and evolution of class VIIIb bHLH family in land plants.

Conclusions

As repeated, dormancy is important for survival of land plants and regulated by integration of various internal and external cues. The regulatory mechanism of dormancy is extensively studied using angiosperms not only in seed but also other vegetative dormant organs including axially bud and underground bulbs, which presented the significant roles of ABA in these phenomena (Pan *et al.*, 2021). The present study identified MpHYP, a critical regulator of gemma dormancy in the liverwort *M. polymorpha*, and presented a limited contribution of ABA in MpHYP-dependent pathway. Given the dramatic and specific effect of Mp*HYP* on gemma dormancy, Mp*HYP* might function as a master regulator. Further investigation would provide new insights into the cooperation of ABA-dependent and -independent pathway, integration of hormonal signals and external cues such as light, and the evolution of class VIIIb bHLH's function in land plants.

Acknowledgements

We appreciate Izumi Yotsui and Yoichi Sakata for providing useful comments on the manuscript. This study was funded by JSPS KAKENHI Grant Numbers JP19H03247 (K.I.), JP20K06680 (D.T).

Author contributions

N.Y., M.Y., A.Y., H.M. and K.T. conducted the experiments. H.K., N.Y., M.Y., A.Y., H.M., K.T., D.T., T.F., Y.K., H.F., T.M., K.I. analyzed the data. H.K. and K.I. designed and supervised the experiments, and wrote the article with contributions of all the authors.

Data availability

RNA-sequence data were deposited at the NCBI in the Sequence Read Archive (SRA) database under the accession numbers DRA013946. The data that support the findings of this study are available from the corresponding author upon reasonable request.

References

Akter K, Kato M, Sato Y, Kaneko Y, Takezawa D. 2014. Abscisic acid-induced rearrangement of intracellular structures associated with freezing and desiccation stress tolerance in the liverwort Marchantia polymorpha. *J Plant Physiol* **171**(15): 1334-1343.

Arnaud N, Girin T, Sorefan K, Fuentes S, Wood TA, Lawrenson T, Sablowski R, Ostergaard L. 2010. Gibberellins control fruit patterning in Arabidopsis thaliana. *Genes Dev* **24**(19): 2127-2132.

Bonnot C, Hetherington AJ, Champion C, Breuninger H, Kelly S, Dolan L. 2019. Neofunctionalisation of basic helix-loop-helix proteins occurred when embryophytes colonised the land. *New Phytol* **223**(2): 993-1008.

Bowman JL. 2016. A Brief History of Marchantia from Greece to Genomics. *Plant Cell Physiol* **57**(2): 210-229.

Bowman JL, Kohchi T, Yamato KT, Jenkins J, Shu S, Ishizaki K, Yamaoka S, Nishihama R, Nakamura Y, Berger F, et al. 2017. Insights into Land Plant Evolution Garnered from the Marchantia polymorpha Genome. *Cell* **171**(2): 287-304.

Corbineau F, Xia Q, Bailly C, El-Maarouf-Bouteau H. 2014. Ethylene, a key factor in the regulation of seed dormancy. *Front Plant Sci* **5**: 539.

de Lucas M, Daviere JM, Rodriguez-Falcon M, Pontin M, Iglesias-Pedraz JM, Lorrain S, Fankhauser C, Blazquez MA, Titarenko E, Prat S. 2008. A molecular framework for light and gibberellin control of cell elongation. *Nature* **451**(7177): 480-484.

Eklund DM, Ishizaki K, Flores-Sandoval E, Kikuchi S, Takebayashi Y, Tsukamoto S, Hirakawa Y, Nonomura M, Kato H, Kouno M, et al. 2015. Auxin Produced by the Indole-3-Pyruvic Acid Pathway Regulates Development and Gemmae Dormancy in the Liverwort Marchantia polymorpha. *Plant Cell* **27**(6): 1650-1669.

Eklund DM, Kanei M, Flores-Sandoval E, Ishizaki K, Nishihama R, Kohchi T, Lagercrantz U, Bhalerao RP, Sakata Y, Bowman JL. 2018. An Evolutionarily Conserved Abscisic Acid Signaling Pathway Regulates Dormancy in the Liverwort Marchantia polymorpha. *Curr Biol* **28**(22): 3691-3699.

Feng S, Martinez C, Gusmaroli G, Wang Y, Zhou J, Wang F, Chen L, Yu L, Iglesias-Pedraz JM, Kircher S, et al. 2008. Coordinated regulation of Arabidopsis thaliana development by light and gibberellins. *Nature* **451**(7177): 475-479.

Furuya T, Shinkawa H, Kajikawa M, Nishihama R, Kohchi T, Fukuzawa H, Tsukaya H. 2021. A plant-specific DYRK kinase DYRKP coordinates cell morphology in Marchantia polymorpha. *J Plant Res* **134**(6): 1265-1277.

Gaillochet C, Jamge S, van der Wal F, Angenent G, Immink R, Lohmann JU. 2018. A molecular network for functional versatility of HECATE transcription factors. *Plant J* **95**(1): 57-70.

Gaillochet C, Stiehl T, Wenzl C, Ripoll JJ, Bailey-Steinitz LJ, Li L, Pfeiffer A, Miotk A, Hakenjos JP, Forner J, et al. 2017. Control of plant cell fate transitions by transcriptional and hormonal signals. *eLife* **6**: e30135.

Girin T, Paicu T, Stephenson P, Fuentes S, Korner E, O'Brien M, Sorefan K, Wood TA, Balanza V, Ferrandiz C, et al. 2011. INDEHISCENT and SPATULA interact to specify carpel and valve margin tissue and thus promote seed dispersal in Arabidopsis. *Plant Cell* **23**(10): 3641-3653.

Gonzalez-Guzman M, Apostolova N, Belles JM, Barrero JM, Piqueras P, Ponce MR, Micol JL, Serrano R, Rodriguez PL. 2002. The short-chain alcohol dehydrogenase ABA2 catalyzes the conversion of xanthoxin to abscisic aldehyde. *Plant Cell* **14**(8): 1833-1846.

Gremski K, Ditta G, Yanofsky MF. 2007. The HECATE genes regulate female reproductive tract development in Arabidopsis thaliana. *Development* **134**(20): 3593-3601.

Hernandez-Garcia J, Sun R, Serrano-Mislata A, Inoue K, Vargas-Chavez C, Esteve-Bruna D, Arbona V, Yamaoka S, Nishihama R, Kohchi T, et al. 2021. Coordination between growth and stress responses by DELLA in the liverwort Marchantia polymorpha. *Curr Biol* **31**(16): 3687-3686.

Inoue K, Nishihama R, Kataoka H, Hosaka M, Manabe R, Nomoto M, Tada Y, Ishizaki K, Kohchi T. 2016. Phytochrome Signaling Is Mediated by PHYTOCHROME INTERACTING FACTOR in the Liverwort Marchantia polymorpha. *Plant Cell* **28**(6): 1406-1421.

Ishikawa M, Murata T, Sato Y, Nishiyama T, Hiwatashi Y, Imai A, Kimura M,

Sugimoto N, Akita A, Oguri Y, et al. 2011. Physcomitrella cyclin-dependent kinase A links cell cycle reactivation to other cellular changes during reprogramming of leaf cells. *Plant Cell* **23**(8): 2924-2938.

Ishizaki K, Chiyoda S, Yamato KT, Kohchi T. 2008. Agrobacterium-mediated transformation of the haploid liverwort Marchantia polymorpha L., an emerging model for plant biology. *Plant Cell Physiol* **49**(7): 1084-1091.

Ishizaki K, Johzuka-Hisatomi Y, Ishida S, Iida S, Kohchi T. 2013. Homologous recombination-mediated gene targeting in the liverwort Marchantia polymorpha L. *Scientific Reports* **3**(1): 1532.

Ishizaki K, Nishihama R, Ueda M, Inoue K, Ishida S, Nishimura Y, Shikanai T, Kohchi T. 2015. Development of Gateway Binary Vector Series with Four Different Selection Markers for the Liverwort Marchantia polymorpha. *PLoS One* **10**(9): e0138876.

Ishizaki K, Nonomura M, Kato H, Yamato KT, Kohchi T. 2012. Visualization of auxin-mediated transcriptional activation using a common auxin-responsive reporter system in the liverwort Marchantia polymorpha. *J Plant Res* **125**(5): 643-651.

Jahan A, Komatsu K, Wakida-Sekiya M, Hiraide M, Tanaka K, Ohtake R, Umezawa T, Toriyama T, Shinozawa A, Yotsui I, et al. 2019. Archetypal Roles of an Abscisic Acid Receptor in Drought and Sugar Responses in Liverworts. *Plant Physiol* **179**(1): 317-328.

Kathare PK, Xu X, Nguyen A, Huq E. 2020. A COP1-PIF-HEC regulatory module fine-tunes photomorphogenesis in Arabidopsis. *Plant J* **104**(1): 113-123.

Kato H, Ishizaki K, Kouno M, Shirakawa M, Bowman JL, Nishihama R, Kohchi T. 2015. Auxin-Mediated Transcriptional System with a Minimal Set of Components Is Critical for Morphogenesis through the Life Cycle in Marchantia polymorpha. *PLoS Genet* **11**(5): e1005084.

Kato H, Kouno M, Takeda M, Suzuki H, Ishizaki K, Nishihama R, Kohchi T. 2017. The Roles of the Sole Activator-Type Auxin Response Factor in Pattern Formation of Marchantia polymorpha. *Plant Cell Physiol* **58**(10): 1642-1651.

Kim D, Paggi JM, Park C, Bennett C, Salzberg SL. 2019. Graph-based genome alignment and genotyping with HISAT2 and HISAT-genotype. *Nature*

Biotechnology **37**(8): 907-915.

Kobayashi Y, Nabeta K, Matsuura H. 2010. Chemical Inhibitors of Viviparous Germination in the Fruit of Watermelon. *Plant and Cell Physiology* **51**(9): 1594-1598.

Komaki S, Sugimoto K. 2012. Control of the plant cell cycle by developmental and environmental cues. *Plant Cell Physiol* **53**(6): 953-964.

Komatsu K, Takezawa D, Sakata Y. 2020. Decoding ABA and osmostress signalling in plants from an evolutionary point of view. *Plant Cell Environ* **43**(12): 2894-2911.

Kubota A, Ishizaki K, Hosaka M, Kohchi T. 2013. Efficient Agrobacterium-mediated transformation of the liverwort Marchantia polymorpha using regenerating thalli. *Biosci Biotechnol Biochem* **77**(1): 167-172.

Li D, Flores-Sandoval E, Ahtesham U, Coleman A, Clay JM, Bowman JL, Chang C. 2020. Ethylene-independent functions of the ethylene precursor ACC in Marchantia polymorpha. *Nat Plants* **6**(11): 1335-1344.

Li H, Handsaker B, Wysoker A, Fennell T, Ruan J, Homer N, Marth G, Abecasis G, Durbin R. 2009. The Sequence Alignment/Map format and SAMtools. *Bioinformatics* **25**(16): 2078-2079.

Li X, Syrkin Wurtele E, Lamotte CE. 1994. Abscisic acid is present in liverworts. *Phytochemistry* **37**(3): 625-627.

Liao Y, Smyth GK, Shi W. 2014. featureCounts: an efficient general purpose program for assigning sequence reads to genomic features. *Bioinformatics* **30**(7): 923-930.

Liljegren SJ, Roeder AH, Kempin SA, Gremski K, Østergaard L, Guimil S, Reyes DK, Yanofsky MF. 2004. Control of fruit patterning in Arabidopsis by INDEHISCENT. *Cell* **116**(6): 843-853.

Liu X, Zhang H, Zhao Y, Feng Z, Li Q, Yang HQ, Luan S, Li J, He ZH. 2013. Auxin controls seed dormancy through stimulation of abscisic acid signaling by inducing ARF-mediated ABI3 activation in Arabidopsis. *Proc Natl Acad Sci U S A* **110**(38): 15485-15490.

Longo C, Holness S, De Angelis V, Lepri A, Occhigrossi S, Ruta V, Vittorioso P. 2020. From the Outside to the Inside: New Insights on the Main Factors That Guide Seed Dormancy and Germination. *Genes (Basel)* **12**(1): 52.

Lujan-Soto E, Dinkova TD. 2021. Time to Wake Up: Epigenetic and Small-RNA-

Mediated Regulation during Seed Germination. *Plants (Basel)* **10**(2): 236.

Ma Y, Szostkiewicz I, Korte A, Moes D, Yang Y, Christmann A, Grill E. 2009. Regulators of PP2C phosphatase activity function as abscisic acid sensors. *Science* **324**(5930): 1064-1068.

Marin E, Nussaume L, Quesada A, Gonneau M, Sotta B, Hugueney P, Frey A, Marion-Poll A. 1996. Molecular identification of zeaxanthin epoxidase of Nicotiana plumbaginifolia, a gene involved in abscisic acid biosynthesis and corresponding to the ABA locus of Arabidopsis thaliana. *Embo j* **15**(10): 2331-2342.

Martin M. 2011. Cutadapt removes adapter sequences from high-throughput sequencing reads. *EMBnet.journal* **17**(1): 10-12.

Masubelele NH, Dewitte W, Menges M, Maughan S, Collins C, Huntley R, Nieuwland J, Scofield S, Murray JA. 2005. D-type cyclins activate division in the root apex to promote seed germination in Arabidopsis. *Proc Natl Acad Sci U S A* **102**(43): 15694-15699.

Nakashima K, Fujita Y, Kanamori N, Katagiri T, Umezawa T, Kidokoro S, Maruyama K, Yoshida T, Ishiyama K, Kobayashi M, et al. 2009. Three Arabidopsis SnRK2 protein kinases, SRK2D/SnRK2.2, SRK2E/SnRK2.6/OST1 and SRK2I/SnRK2.3, involved in ABA signaling are essential for the control of seed development and dormancy. *Plant Cell Physiol* **50**(7): 1345-1363.

Née G, Kramer K, Nakabayashi K, Yuan B, Xiang Y, Miatton E, Finkemeier I, Soppe WJJ. 2017. DELAY OF GERMINATION1 requires PP2C phosphatases of the ABA signalling pathway to control seed dormancy. *Nat Commun* **8**(1): 72.

Nishimura N, Tsuchiya W, Moresco JJ, Hayashi Y, Satoh K, Kaiwa N, Irisa T, Kinoshita T, Schroeder JI, Yates JR, 3rd, et al. 2018. Control of seed dormancy and germination by DOG1-AHG1 PP2C phosphatase complex via binding to heme. *Nat Commun* **9**(1): 2132.

Pan W, Liang J, Sui J, Li J, Liu C, Xin Y, Zhang Y, Wang S, Zhao Y, Zhang J, et al. 2021. ABA and Bud Dormancy in Perennials: Current Knowledge and Future Perspective. *Genes (Basel)* **12**(10): 1635.

Park SY, Fung P, Nishimura N, Jensen DR, Fujii H, Zhao Y, Lumba S, Santiago J, Rodrigues A, Chow TF, et al. 2009. Abscisic acid inhibits type 2C protein

phosphatases via the PYR/PYL family of START proteins. *Science* **324**(5930): 1068-1071.

Perreau F, Frey A, Effroy-Cuzzi D, Savane P, Berger A, Gissot L, Marion-Poll A. 2020. ABSCISIC ACID-DEFICIENT4 Has an Essential Function in Both cis-Violaxanthin and cis-Neoxanthin Synthesis. *Plant Physiol* **184**(3): 1303-1316.

Robinson MD, McCarthy DJ, Smyth GK. 2009. edgeR: a Bioconductor package for differential expression analysis of digital gene expression data. *Bioinformatics* **26**(1): 139-140.

Saint-Marcoux D, Proust H, Dolan L, Langdale JA. 2015. Identification of reference genes for real-time quantitative PCR experiments in the liverwort Marchantia polymorpha. *PLoS One* **10**(3): e0118678.

Sano N, Marion-Poll A. 2021. ABA Metabolism and Homeostasis in Seed Dormancy and Germination. *Int J Mol Sci* **22**(10): 5069.

Saruhashi M, Kumar Ghosh T, Arai K, Ishizaki Y, Hagiwara K, Komatsu K, Shiwa Y, Izumikawa K, Yoshikawa H, Umezawa T, et al. 2015. Plant Raf-like kinase integrates abscisic acid and hyperosmotic stress signaling upstream of SNF1-related protein kinase2. *Proc Natl Acad Sci U S A* **112**(46): E6388-6396.

Schena M, Lloyd AM, Davis RW. 1991. A steroid-inducible gene expression system for plant cells. *Proc Natl Acad Sci U S A* **88**(23): 10421-10425.

Schuster C, Gaillochet C, Lohmann JU. 2015. Arabidopsis HECATE genes function in phytohormone control during gynoecium development. *Development* **142**(19): 3343-3350.

Schuster C, Gaillochet C, Medzihradszky A, Busch W, Daum G, Krebs M, Kehle A, Lohmann JU. 2014. A regulatory framework for shoot stem cell control integrating metabolic, transcriptional, and phytohormone signals. *Dev Cell* **28**(4): 438-449.

Schwartz SH, Tan BC, Gage DA, Zeevaart JAD, McCarty DR. 1997. Specific Oxidative Cleavage of Carotenoids by VP14 of Maize. *Science* **276**(5320): 1872-1874.

Seo M, Peeters AJ, Koiwai H, Oritani T, Marion-Poll A, Zeevaart JA, Koornneef M, Kamiya Y, Koshiba T. 2000. The Arabidopsis aldehyde oxidase 3 (AAO3) gene product catalyzes the final step in abscisic acid biosynthesis in leaves. *Proc Natl*

Acad Sci U S A **97**(23): 12908-12913.

Shimamura M. 2016. Marchantia polymorpha: Taxonomy, Phylogeny and Morphology of a Model System. *Plant Cell Physiol* **57**(2): 230-256.

Sugano SS, Nishihama R, Shirakawa M, Takagi J, Matsuda Y, Ishida S, Shimada T, Hara-Nishimura I, Osakabe K, Kohchi T. 2018. Efficient CRISPR/Cas9-based genome editing and its application to conditional genetic analysis in Marchantia polymorpha. *PLoS One* **13**(10): e0205117.

Tian F, Yang D-C, Meng Y-Q, Jin J, Gao G. 2019. PlantRegMap: charting functional regulatory maps in plants. *Nucleic Acids Research* **48**(D1): D1104-D1113.

Tougane K, Komatsu K, Bhyan SB, Sakata Y, Ishizaki K, Yamato KT, Kohchi T, Takezawa D. 2010. Evolutionarily conserved regulatory mechanisms of abscisic acid signaling in land plants: characterization of ABSCISIC ACID INSENSITIVE1-like type 2C protein phosphatase in the liverwort Marchantia polymorpha. *Plant Physiol* **152**(3): 1529-1543.

Trapnell C, Williams BA, Pertea G, Mortazavi A, Kwan G, van Baren MJ, Salzberg SL, Wold BJ, Pachter L. 2010. Transcript assembly and quantification by RNA-Seq reveals unannotated transcripts and isoform switching during cell differentiation. *Nature Biotechnology* **28**(5): 511-515.

Umezawa T, Sugiyama N, Mizoguchi M, Hayashi S, Myouga F, Yamaguchi-Shinozaki K, Ishihama Y, Hirayama T, Shinozaki K. 2009. Type 2C protein phosphatases directly regulate abscisic acid-activated protein kinases in Arabidopsis. *Proc Natl Acad Sci U S A* **106**(41): 17588-17593.

Vlad F, Rubio S, Rodrigues A, Sirichandra C, Belin C, Robert N, Leung J, Rodriguez PL, Lauriere C, Merlot S. 2009. Protein phosphatases 2C regulate the activation of the Snf1-related kinase OST1 by abscisic acid in Arabidopsis. *Plant Cell* **21**(10): 3170-3184.

Yasui Y, Tsukamoto S, Sugaya T, Nishihama R, Wang Q, Kato H, Yamato KT, Fukaki H, Mimura T, Kubo H, et al. 2019. GEMMA CUP-ASSOCIATED MYB1, an Ortholog of Axillary Meristem Regulators, Is Essential in Vegetative Reproduction in Marchantia polymorpha. *Curr Biol* **29**(23): 3987-3995.

Zhu L, Xin R, Bu Q, Shen H, Dang J, Huq E. 2016. A Negative Feedback Loop between PHYTOCHROME INTERACTING FACTORs and HECATE Proteins Fine-

Tunes Photomorphogenesis in Arabidopsis. *Plant Cell* **28**(4): 855-874.

Figure legends

Fig. 1 Mp*HYP* plays critical role in gemma dormancy. (a) Relative expression of Mp*HYP* to Mp*EF1α*. Samples were collected from 1-week-old whole thallus (TH), and midrib (MR) or gemma cup (GC) of 3-week-old thallus. Expression level was normalized to TH. Bars or circles indicate mean values or each data point, respectively. (b) Gene structure of Mp*HYP*. White and black boxes represent UTR and CDS, respectively. Mp*HYP* does not have any introns. Blue and red bars indicate the region encoding bHLH domain and that recombined in Mp*hyp*^{ko} mutants (see also Fig. S1a). (c) Top and side view of 1-week-old gemmalings of WT, MphypKO, and *g*Mp*HYP*/Mp*hyp*^{ko}. Bars = 1 mm. (d) Gemma cups and gemmae from 4-week-old thallus of WT or Mp*hyp*^{ko}. Gray images were taken with SEM. The arrow indicates the elongated rhizoids. Bars = 0.5 mm. (e) Germination rate of gemma from WT (Tak-1), Mp*hyp*^{ko}, and gMp*HYP*/Mp*hyp*^{ko} lines at 17-day-old stage. Bars or dots indicate mean values or each data point, respectively.

Fig. 2 GUS staining of Mp*HYP*$_{pro}$*:GUS*. (a-c) 5- (a), 10- (b), and 14-day-old (c) gemmalings of Mp*HYP*$_{pro}$*:GUS*. (d,e) Section image of gemma cup. Black square indicates the region magnified in (e). (f) Mature gemma before germination. Bars = 2 mm (a-c), 0.1 mm (d-f).

Fig. 3 Overexpression of Mp*HYP* represses gemma germination and thallus growth. (a) Expression analysis of Mp*HYP* in Tak-1 (WT) and Mp*HYP-GR* plants by qRT-PCR. RNA samples were collected from 1-week-old gemmalings. Expression level was normalized to WT. Bars or dots indicate mean values or each data point, respectively. (b,c) Gemmae (b) or 7-day-old gemmalings (c) of Mp*HYP-GR* were grown in mock (M) or 10 μM DEX (D) conditions. The number indicates the days of each treatment. For example, M7D7 means that plants were grown for 7 days in mock condition, followed by 7-day cultivation on the medium with DEX. Insets indicate images in the same magnification as in mock condition at same age. Scale bars = 0.5 mm (b), 2 mm (c).

Fig. 4 Transcriptome analysis using Mp*hyp*^{ko} and Mp*HYP-GR*. (a) PC analysis plot of RNA-seq data from gemma cups of WT and Mp*hyp*^{ko}, and 7-day-old gemmalings of

Mp*HYP-GR* treated with mock or DEX condition for 2 or 24 h. Circles with the same color indicate biological replicates for the same conditions. (b) Venn diagrams of DEGs between each comparison. The number of genes classified in each group is indicated. (c) GO term enrichment analysis using the 413 MpHYP-repressed genes. (d) Expression analysis of Mp*CYCD;1* gene by qRT-PCR. 7-day-old gemmalings of Mp*HYP-GR* were treated with or without 10 μM DEX and/or 10 μM CHX for 2 h. Bars or circles indicate mean values or each data point (n=3), respectively. Small letters indicate significant differences ($p < 0.01$ by ANOVA followed by Tukey's HSD test). (e) EdU incorporation assay to visualize S-phase progression in Mp*HYP-GR*. 3-day-old gemmalings were incubated with or without 10 μM DEX for 6 h, and then cultured on the medium containing EdU for 1 h. Images of EdU (red) and cell wall (gray) were merged. Scale bars = 100 μm. (f) EdU-positive cells per notch were counted from the confocal microscopy images (e). Bars or circles indicate mean values or each data point (n = 7), respectively. Small letters indicate significant differences ($p < 0.01$ by ANOVA followed by Tukey's HSD test).

Fig. 5 The relationship between Mp*HYP* and ABA pathway. (a) Time course qRT-PCR experiments for Mp*NCED*, Mp*ABA4*, Mp*LAEL1*, and Mp*LAEL5* in Mp*HYP-GR*. 7-day-old gemmalings were treated with 10 μM DEX for 0, 2, 4, or 6 h. Expression level was normalized to 0 h. Lines or dots indicate mean values or each data point, respectively. (b) qRT-PCR experiments for Mp*NCED* and Mp*LEAL5* in 7-day-old Mp*HYP-GR* thalli with or without 10 μM DEX and/or 10 μM CHX treatment for 2 h. Small letters indicate significant differences ($p < 0.05$ by ANOVA followed by Tukey's HSD test, n = 3). (c, d) Quantification of ABA content in gemmae of WT and Mphyp^{ko} and gMpHYP/ Mphyp^{ko} (c), and those in 1-week-old thallus of MpHYP-GR with or without 10 μM DEX treatment for 24 h (d). (e) Germination rate of gemmae in gemma cups of WT, Mphyp^{ko}, Mp*pyl1* and Mp*nced* mutants at 17-day-old gemmaling stage. (f) 7-day-old gemmalings of Tak-1, Mp*HYP-GR* and Mp$pyl1^{ge}$/Mp*HYP-GR* grown without or with 10 μM DEX. Bars or circles indicate mean values or each data point, respectively (a-e). Small letters indicate significant differences ($p < 0.05$ (a, b, g), 0.01 (c-f) by ANOVA followed by Tukey's HSD test).

Supporting information

Fig. S1. Knock-out of Mp*HYP* with homologous recombination.

Fig. S2 Mutagenesis in Mp*NCED* by CRISPR/Cas9 method.

Fig. S3 Generation of Mp*pyl1*^{ge}/Mp*HYP-GR* by CRISPR/Cas9 system.

Table S1. Primers used in this study.

Table S2. RNA-seq results of cell cycle-related genes.

Table S3. RNA-seq results of ethylene-related genes.

Table S4. RNA-seq results of auxin-related genes.

Table S5. RNA-seq results of ABA-related genes.

Table S6. RNA-seq results of Mp*LEAL* genes.

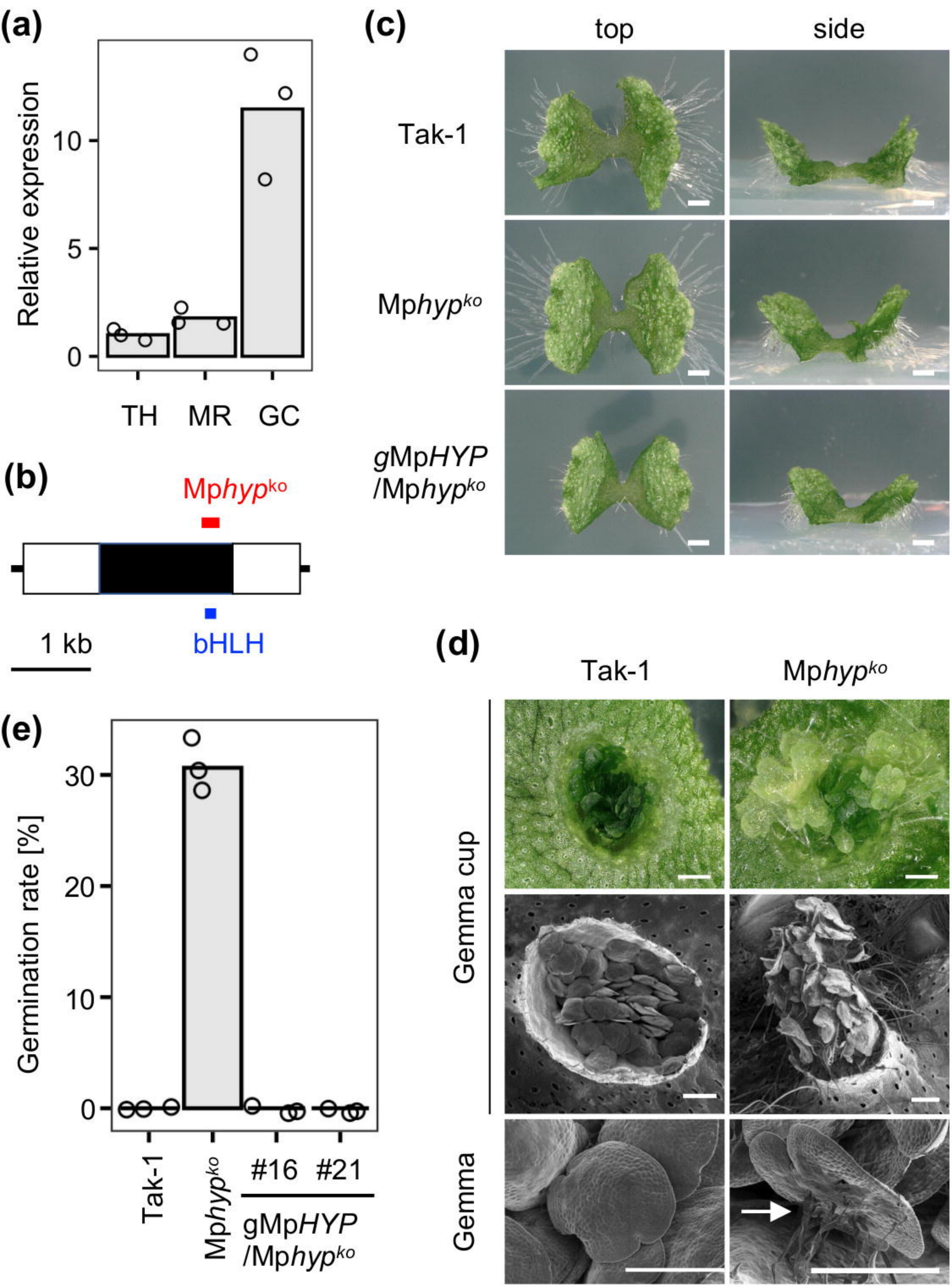
(a)
Relative expression
10
5
0
TH
MR
GC
(b)
Mphypko
1 kb
bHLH
(c)
top
side
Tak-1
Mphypko
gMpHYP
/Mphypko
(d)
Tak-1
Mphypko
Gemma cup
Gemma
(e)
Germination rate [%]
30
20
10
0
Tak-1
Mphypko
#16
#21
gMpHYP
/Mphypko

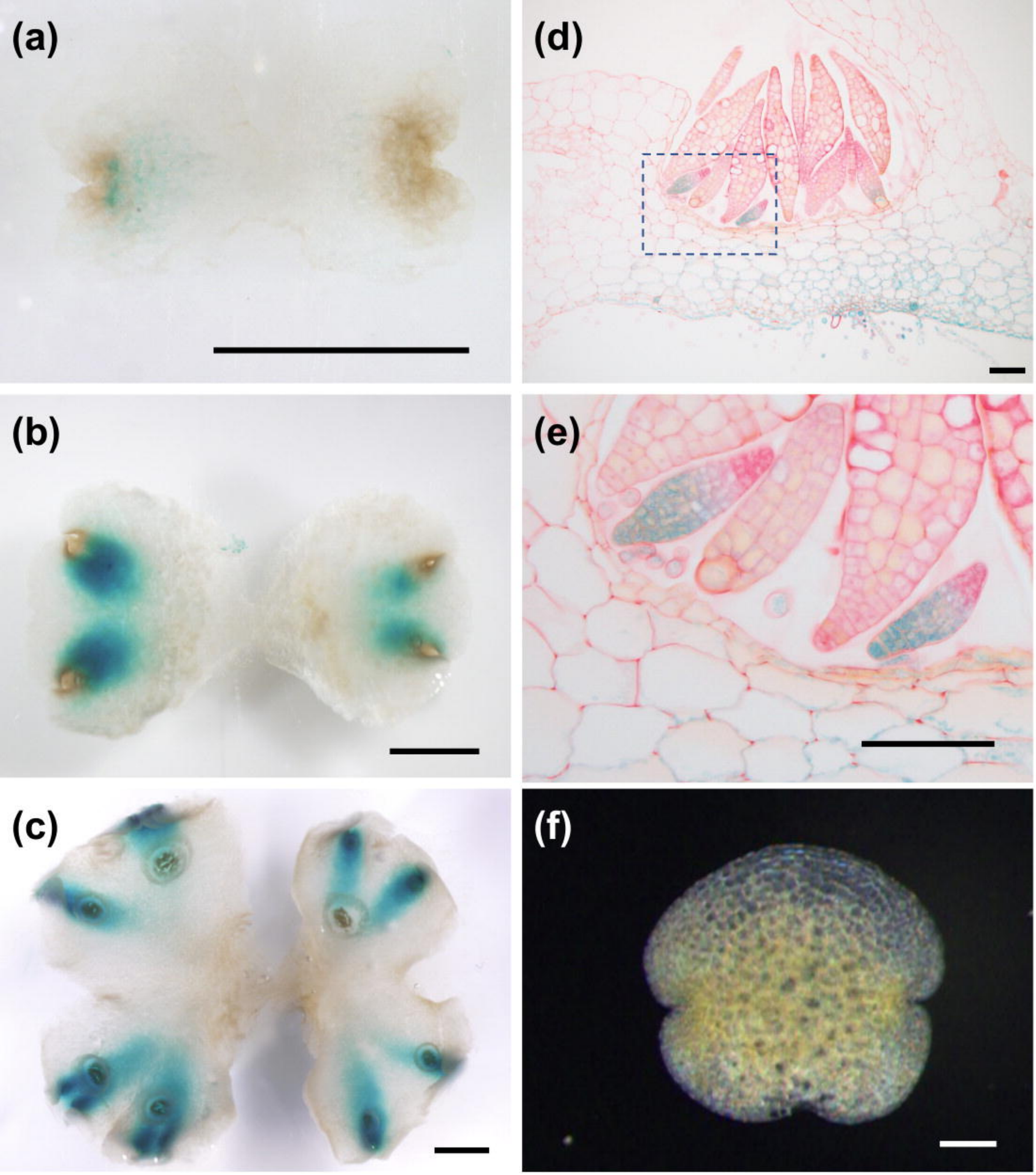
(a)
(b)
(c)
(d)
(e)
(f)

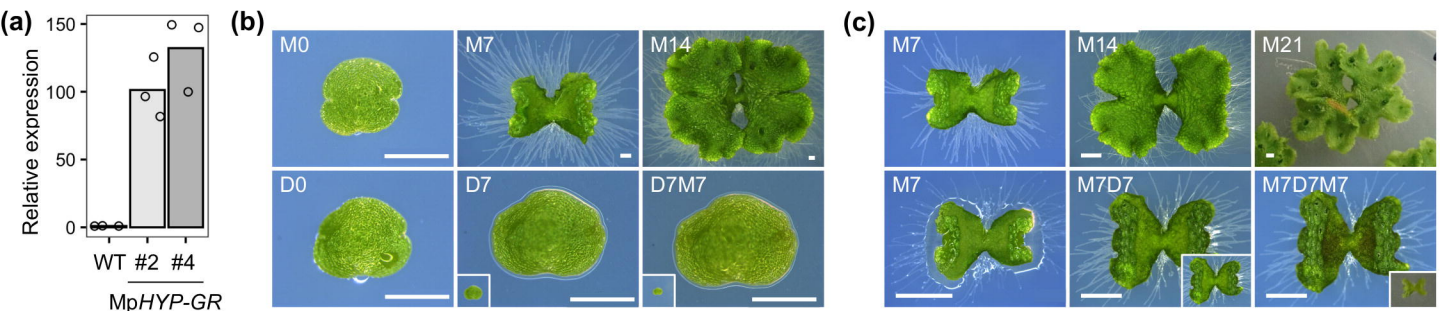
(a)
Relative expression
150
100
50
0
WT
#2
#4
MpHYP-GR
(b)
M0
M7
M14
D0
D7
D7M7
(c)
M7
M14
M21
M7
M7D7
M7D7M7

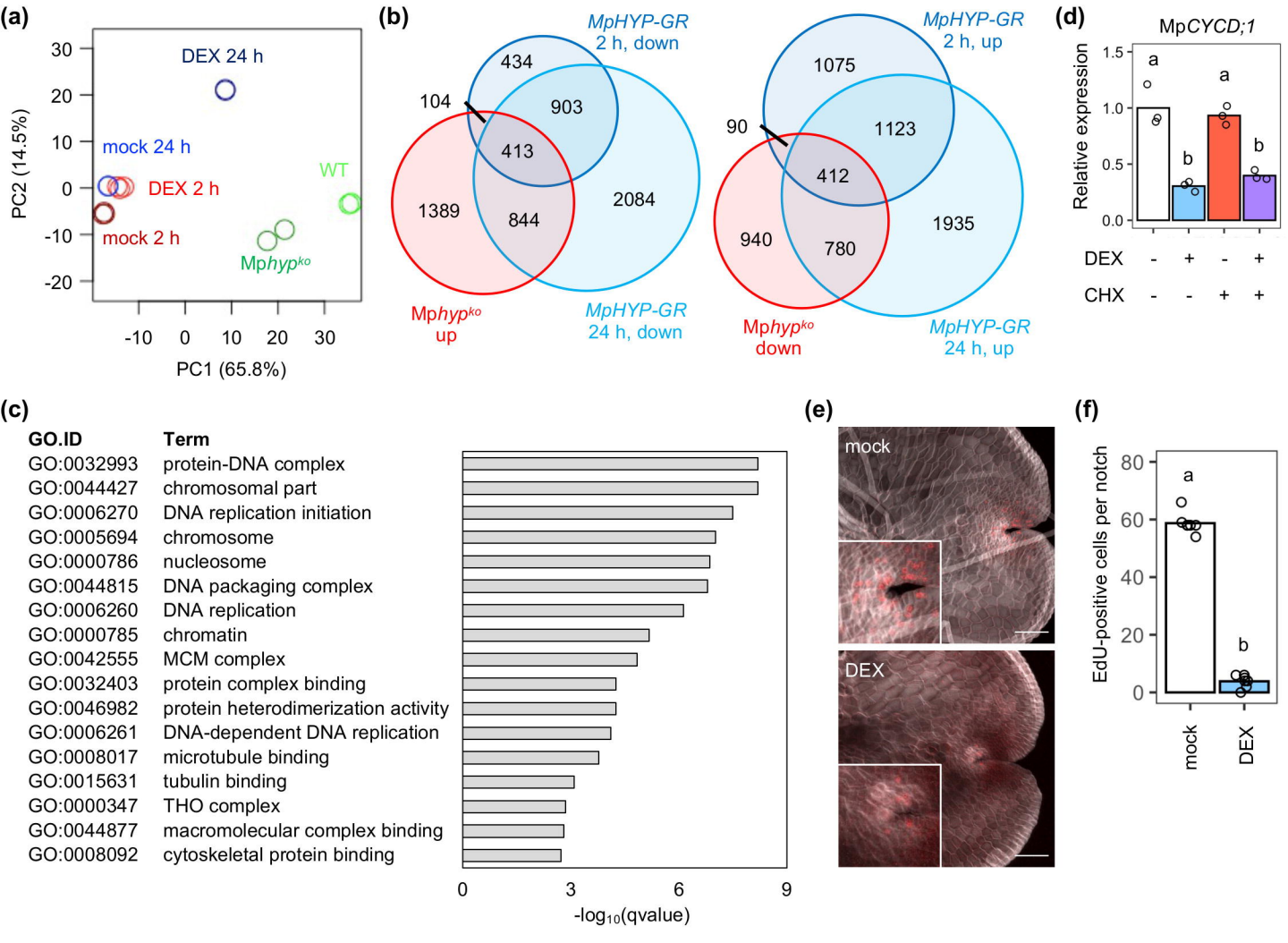
(a)
DEX 24 h
mock 24 h
DEX 2 h
mock 2 h
WT
Mphypko
PC2 (14.5%)
PC1 (65.8%)
(b)
MpHYP-GR 2 h, down
434
903
104
413
1389
844
2084
Mphypko up
MpHYP-GR 24 h, down
MpHYP-GR 2 h, up
1075
1123
90
412
940
780
1935
Mphypko down
MpHYP-GR 24 h, up
(d)
MpCYCD;1
Relative expression
DEX
CHX
(c)
GO.ID
Term
GO:0032993 protein-DNA complex
GO:0044427 chromosomal part
GO:0006270 DNA replication initiation
GO:0005694 chromosome
GO:0000786 nucleosome
GO:0044815 DNA packaging complex
GO:0006260 DNA replication
GO:0000785 chromatin
GO:0042555 MCM complex
GO:0032403 protein complex binding
GO:0046982 protein heterodimerization activity
GO:0006261 DNA-dependent DNA replication
GO:0008017 microtubule binding
GO:0015631 tubulin binding
GO:0000347 THO complex
GO:0044877 macromolecular complex binding
GO:0008092 cytoskeletal protein binding
-log10(qvalue)
(e)
mock
DEX
(f)
EdU-positive cells per notch
mock
DEX

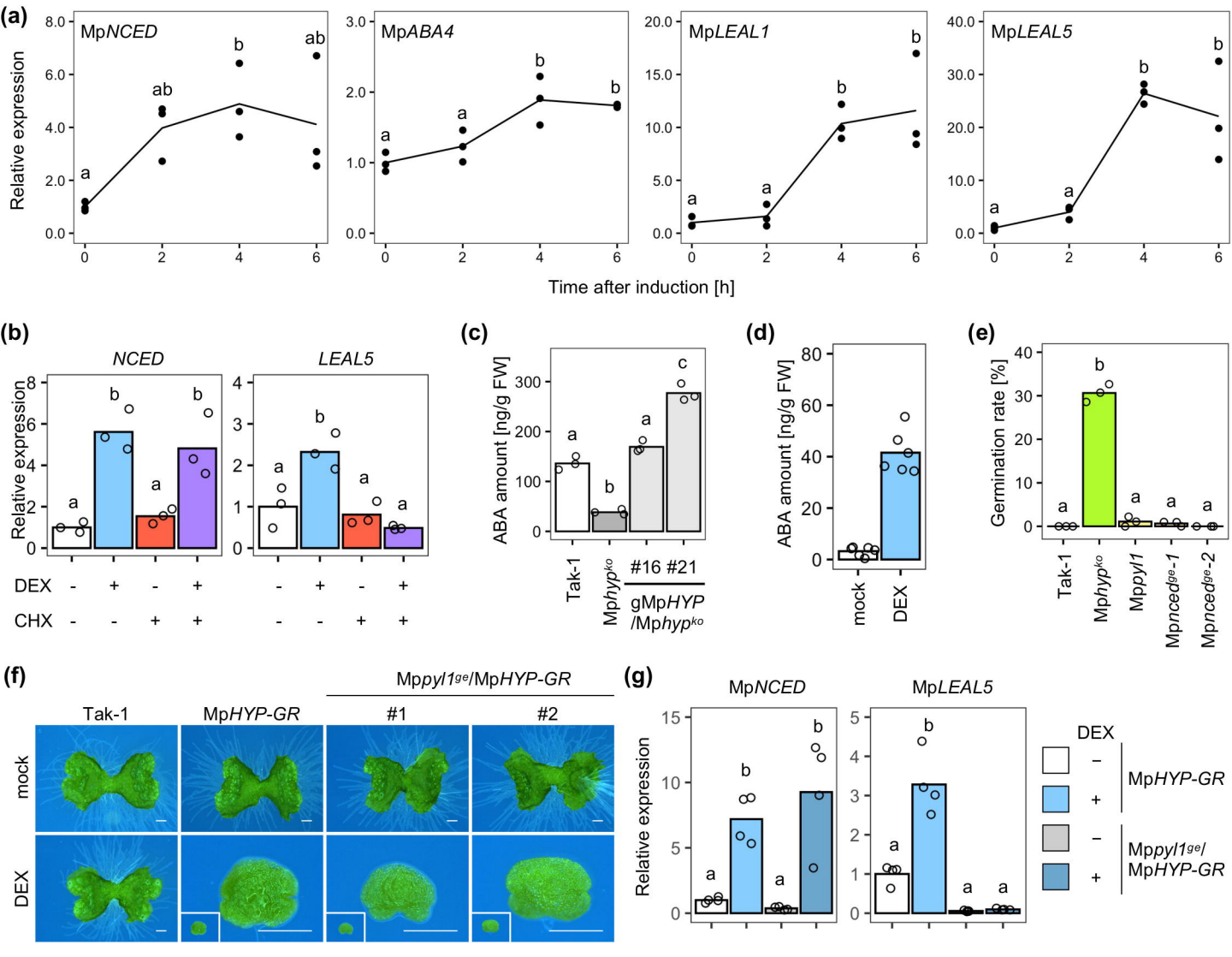
(a)
MpNCED
MpABA4
MpLEAL1
MpLEAL5
Relative expression
Time after induction [h]
(b)
NCED
LEAL5
Relative expression
DEX
CHX
(c)
ABA amount [ng/g FW]
Tak-1
Mphypko
#16 #21
gMpHYP /Mphypko
(d)
ABA amount [ng/g FW]
mock
DEX
(e)
Germination rate [%]
Tak-1
Mphypko
Mppyl1
Mpncedge-1
Mpncedge-2
(f)
Mppyl1ge/MpHYP-GR
Tak-1
MpHYP-GR
#1
#2
mock
DEX
(g)
MpNCED
MpLEAL5
Relative expression
DEX
MpHYP-GR
Mppyl1ge/ MpHYP-GR